# Supporting Information

## Derrington et al. 10.1073/pnas.1001831107

### SI Text

**Translocation Analysis Method.** All software was custom designed in Matlab (The Mathworks). Translocation of DNA were first identified using current-thresholds as described in Butler (1). Minor variations in open-pore current levels were seen across a number of experiments and were likely due to minor changes in buffer conditions influencing conductivity. The fluctuations between experiments were minimized by dividing the residual current for each translocation by the surrounding unblocked current level. To report values in current, we multiplied these normalized-currents by the average open-pore current $325.1 \pm 1.8$ pA (mean $\pm$ s.e.m.) for an applied voltage of 180 mV and $252.2 \pm -3.0$ for 140 mV applied voltage. Histograms of averaged residual currents were constructed using translocation with an average $I_{res} < 0.5^{*}I_{OS}$ and with a duration longer than 1 ms. Histograms in the main text are chosen from individual experiments that closely match the most frequent residual current when averaged over multiple experiments, as recorded in Tables S1 and S2.

Translocations of DNA used to explore DI sequencing were initially identified as in Butler (1) and normalized by the surrounding open-pore current. The residual currents were then Gaussian filtered at 4 kHz and down sampled at 20 kHz and further processed with a 20-point median filter. We identified transitions between current levels with custom edge detection software utilizing a gradient threshold to detect transitions between unique levels. We used the local maxima of the current gradient to locate possible transitions. To be considered unique, levels within residual current traces were required to satisfy several conditions: level durations must be longer than 1.5 ms, each level's average current must be separated by both more than 3.8 pA from surrounding levels and by more than 1.5 times the quadrature sum of surrounding levels current fluctuation. If these requirements were not met, the levels were combined until possible levels were determined as unique. Residual current traces with four (or five in the case of the blind 3′-GTCAC-5′ sequence) levels were found to follow patterns as seen in Figs. S2, S3, and S4. Averages of these levels can be found in Tables S3, S4, and S5. Information for events with fewer than four (or five) events is summarized in Tables S3, S4, and S5.

**Qualitative Barrier Model.** The data, shown in Fig. S1, show the effect of substituting a nucleotide $dN_x$ at a position $x = 1,2,3$ following the duplex terminus of a hairpin DNA. The nucleotides are substituted in poly-dA, poly-dC, or poly-dT homopolymer tails. We observe that the presence of $dC_x$ or a $dT_x$ substitution in poly-dA, causes the residual current to change toward the homopolymer value $I_{dC}$ and $I_{dT}$, respectively. The substitutions of a $dA_x$ nucleotide in either poly-dC or poly-dT homopolymers do not consistently alter the current. It is possible that a qualitative model could describe this data.

It may be natural to expect each of these nucleotides to act like a resistor impeding the ionic flow. Our data are not self-consistent with this description, as has been observed in α-hemolysin (2). Instead of a resistor model, we postulate that each the amino acid residues within the constriction combined with the nucleotides in the constriction of MspA form a unique barrier to ion current. The presence of particular nucleotides, such as dC, dT, may induce a rate limit to the ion transport. Here we discuss how our data are consistent with this model.

With this model in mind, the observation that $I_{dC} < I_{dA}$ suggests that any dC nucleotide will present a higher barrier than dA nucleotides to ion transport. When a single $dC_x$ is put in poly-dA, the residual current is reduced by a rate-limit induced by the $dC_x$ barrier. The reduction in current due the $dC_x$ insertion is strongest at $x = 2$, and somewhat less strong at $x = 1$, likely because these locations would place the substitution in the narrowest part of MspA's constriction. When we examine the influence of a $dA_x$ substitution in poly-dC tails, we see that the current is not appreciably increased. This is because the high-barrier dC nucleotides surrounding the $dA_x$ substitution induce a rate limit to the ion transport while the smaller barrier presented by the single dA cannot undo this rate limit.

We see a similar effect when the high barrier caused by dT is put in a poly-dA tail: The current is considerably reduced as the substitution $dT_x$ is located inside the constriction, particularly at $x = 1$. As $I_{dT} < I_{dA}$, these observation support the possibility that specific nucleotides induce rate limits to ion flow. Further implications of this model indicate when the substitution $dA_1$ is made in poly-dT, the dT at the second position will be the next nucleotide available to induce a rate-limit to ionic transport. As would be expected, we see that the $dT_2$ substitution in poly-dA induces a rate-limited current with distribution similar to current due to the $dA_1$ substitution in poly-dT. The difference in which location the substitution $dC_x$ and $dT_x$ is most influential in poly-dA ($x = 2$, and $x = 1$, respectively), may be attributed to the specific interactions between the nucleotides with the pore and the hairpin terminus.

Rate-limiting models have been proposed to explain the ionic flow in other pores absent of DNA (3, 4). We intend to further investigate the plausibility of this model with additional experiments and with MD-simulation.


1. Butler TZ, Pavlenok M, Derrington IM, Niederweis M, & Gundlach JH (2008) Single-molecule DNA detection with an engineered MspA protein nanopore. *Proc Natl Acad Sci USA* 105:20647–20652.
2. Purnell RF & Schmidt JJ (2009) Discrimination of single base substitutions in a DNA strand immobilized in a biological nanopore. *ACS Nano* 3(9):2533–2538.
3. Läuger P (1973) Ion transport through pores: A rate-theory analysis. *BBA-Biomembranes* 311(3):423–441.
4. Hille B (2001) Ionic channels of excitable membranes. (Sinauer Associates, Sunderland, MA).

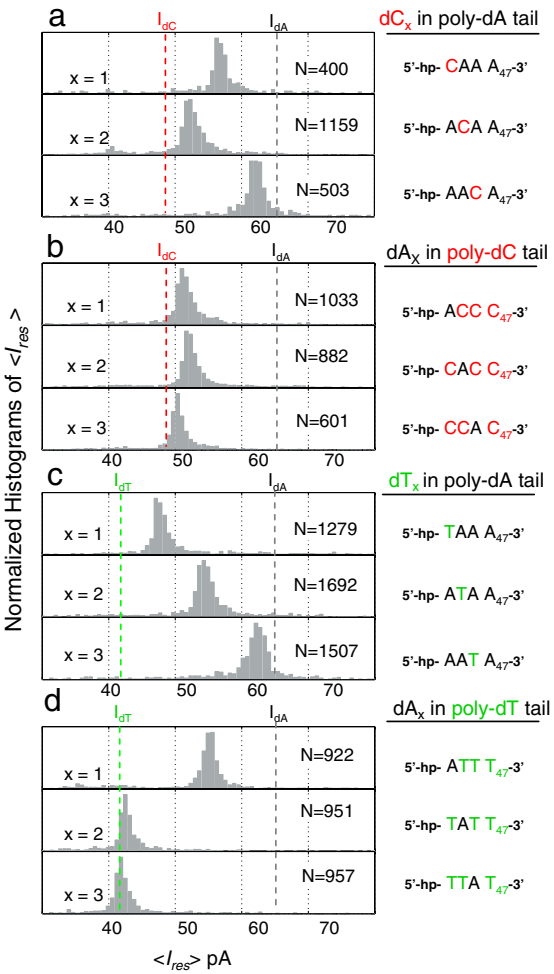


**Fig. S1.** Influence of single nucleotide substitutions in homopolymer backgrounds. Histograms representative of the average residual current, $\langle I_{res} \rangle$ for a nucleotide dN insertions in homopolymer hairpin tails at position *x* away from the hairpin duplex, denoted dN$_x$. Vertical dashed lines indicate the Gaussian mean of the indicated homopolymer residual currents. Counts for each histogram are given by *N*. Note the effect of the homopolymer background on the effect of the nucleotide substitution This is discussed in *SI Text*.

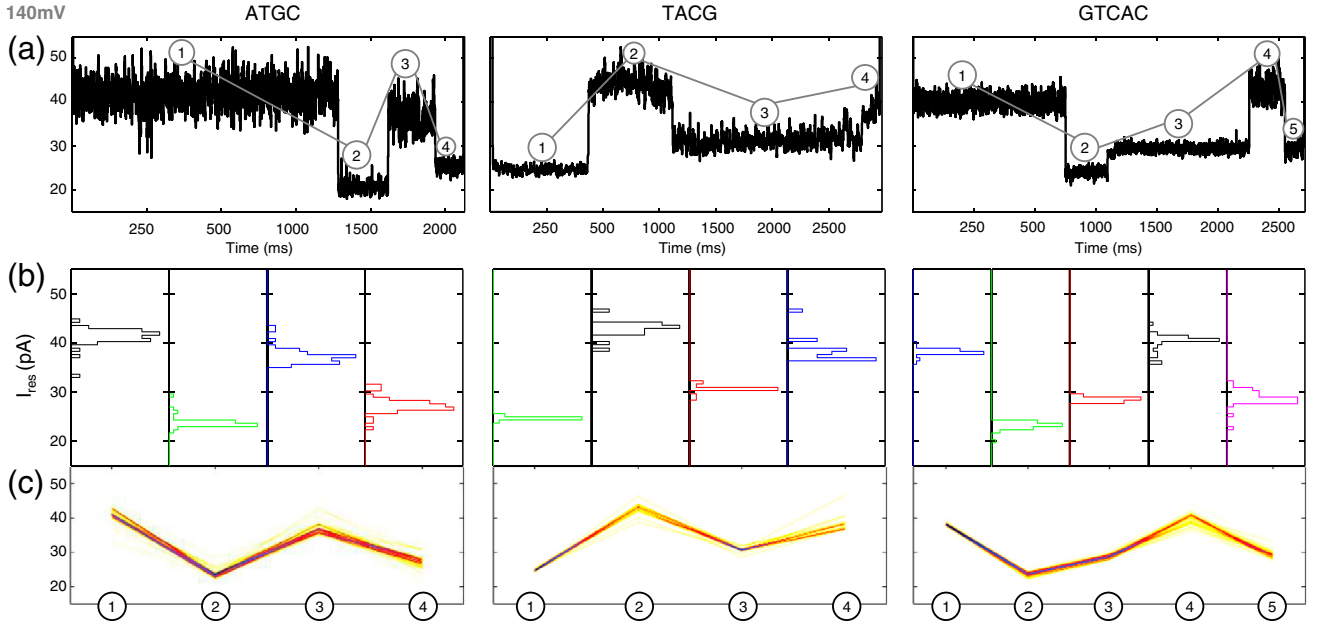


**Fig. S2.** Data from DI-sequencing examples for analyte DNA, 3′ATGC5′ (left column), 3′ TACG 5′ (middle column), and blind DNA determined to be 3′ GTCAC 5′ (right column) at applied voltage of 140 mV. Each group of figures contains: (*A*) an example current trace containing four (or five) levels, (*B*) histograms for each of the average current for each level from multiple events with four (or five) levels, and (*C*) a density plot indicating the transition between the current levels for the multiple events in the histograms. Unblocked pore current was 237.0 ± 1.0 pA (mean ± s.e.m.). Three or greater individual experiments with each DI-DNA were performed. Additional information may be found in Tables S3, S4, and S5.

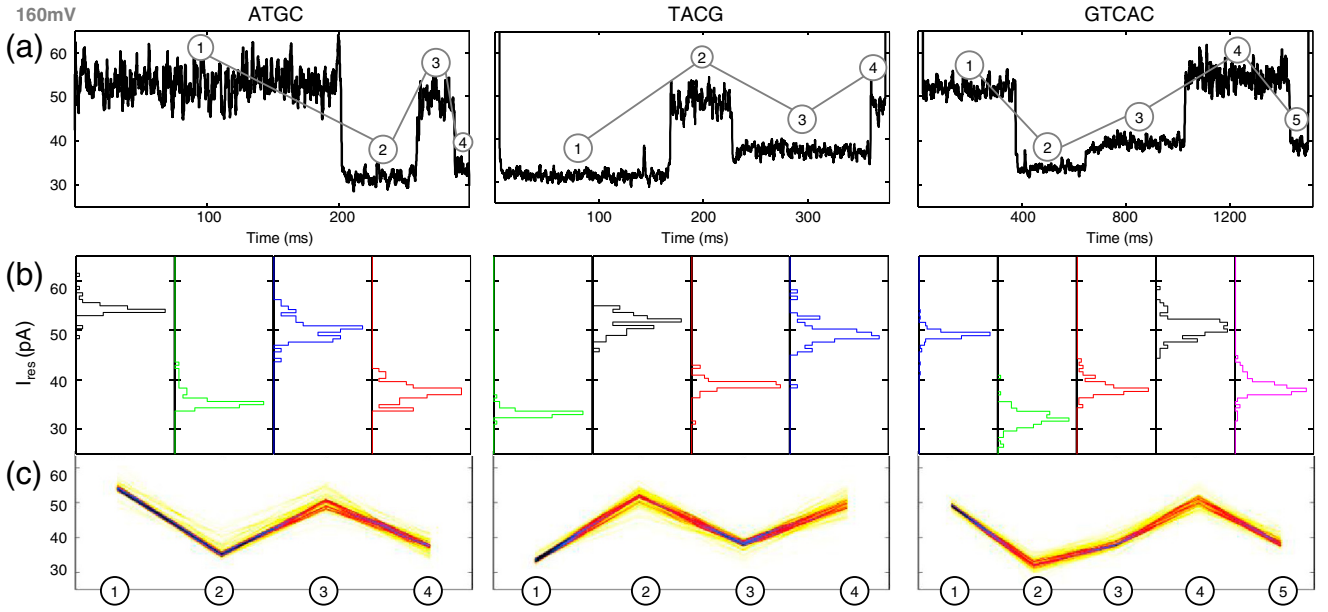


**Fig. S3.** Same as Fig. S2 but for an applied voltage of 160 mV. The unblocked pore current was 294.7 ± 0.8 pA (mean ± s.e.m.).

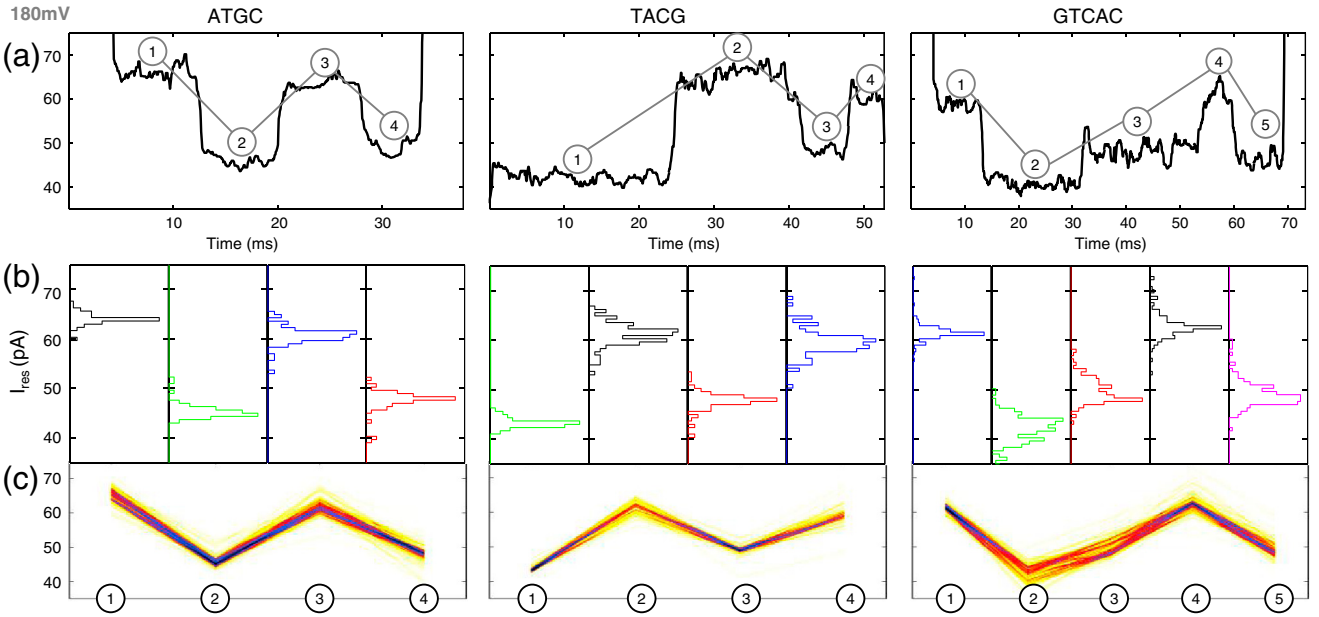


**Fig. S4.** Same as Fig. S2 but for an applied voltage of 180 mV. The unblocked pore current was 325.1 ± 1.8 pA (mean ± s.e.m.). At higher voltage it becomes more difficult to distinguish unique levels in current traces because of the reduced time-averaging of current levels.

**Table S1. Information for hairpin DNA with different tails examined with MspA**

| Duplex | Hairpin Sequences | mean of Gauss mean of $I_{res}$ | mean of Gauss width of $I_{res}$ | s.e.m. of Gauss means | # transloc. | # exp |
|---|---|---|---|---|---|---|
| 5′ GCT GGC TCT GTT GCT CTC TCG CAA CAG AGC CAG C | (14 bp, 64% GC) | (pA) | (pA) | (pA) | | |
| **TAIL** | | | | | | |
| $(dA)_{50}$: | AAA AAA AAA AAA AAA AAA AAA AAA AAA AAA AAA AAA AAA AAA AAA AAA AAA AA 3′ | 65.5 | 1.5 | 1.0 | 3257 | 7 |
| $(dC)_{50}$: | CCC CCC CCC CCC CCC CCC CCC CCC CCC CCC CCC CCC CCC CCC CCC CCC CCC CC 3′ | 48.4 | 1.1 | 1.4 | 1830 | 8 |
| $(dT)_{50}$: | TTT TTT TTT TTT TTT TTT TTT TTT TTT TTT TTT TTT TTT TTT TTT TTT TTT TT 3′ | 41.9 | 1.2 | 1.1 | 2407 | 4 |
| $(dG)_3(dA)_{47}$: | GGG AAA AAA AAA AAA AAA AAA AAA AAA AAA AAA AAA AAA AAA AAA AAA AAA AA 3′ | 59.4 | 1.2 | 0.8 | 2938 | 5 |
| $(dC)_4(dA)_{46}$: | CCC CAA AAA AAA AAA AAA AAA AAA AAA AAA AAA AAA AAA AAA AAA AAA AAA AA 3′ | 50.0 | 0.9 | 1.1 | 914 | 4 |
| $(dA)_3(dC)_4(dA)_{43}$: | AAA CCC CAA AAA AAA AAA AAA AAA AAA AAA AAA AAA AAA AAA AAA AAA AAA AA 3′ | 65.4 | 1.3 | 1.7 | 1186 | 2 |
| $(dA)_6(dC)_4(dA)_{40}$: | AAA AAA CCC CAA AAA AAA AAA AAA AAA AAA AAA AAA AAA AAA AAA AAA AAA AA 3′ | 65.7 | 1.7 | 2.1 | 1094 | 3 |
| $(dA)_3$ rand1: | AAA TAC GCA TAC ATC CTA AGA ACT CAG ACT ACC TCC CAA TAA ATC CAC AC 3′ | 64.1 | 1.5 | 0.5 | 1073 | 3 |
| $(dA)_3$ rand2: | AAA TCA GAC TAC CTC CCA ATA AAT CCG CAG CAA TCC TCA CAC CTA ATA AT 3′ | 65.6 | 1.6 | 0.5 | 822 | 3 |
| $(dC)_3$ rand1: | CCC TAC GCA TAC ATC CTA AGA ACT CAG ACT ACC TCC CAA TAA ATC CAC AC 3′ | 48.6 | 0.8 | 0.2 | 1319 | 4 |
| $(dC)_3$ rand2: | CCC TCA GAC TAC CTC CCA ATA AAT CCG CAG CAA TCC TCA CAC CTA ATA AT 3′ | 48.6 | 0.9 | 0.6 | 1325 | 4 |
| $dC(dA)_{49}$: | CAA AAA AAA AAA AAA AAA AAA AAA AAA AAA AAA AAA AAA AAA AAA AAA AAA AA 3′ | 56.9 | 1.7 | 2.0 | 3198 | 6 |
| $dAdC(dA)_{48}$: | ACA AAA AAA AAA AAA AAA AAA AAA AAA AAA AAA AAA AAA AAA AAA AAA AAA AA 3′ | 52.1 | 1.2 | 0.3 | 2597 | 3 |
| $(dA)_2dC(dA)_{47}$: | AAC AAA AAA AAA AAA AAA AAA AAA AAA AAA AAA AAA AAA AAA AAA AAA AAA AA 3′ | 61.4 | 1.3 | 0.4 | 1550 | 2 |
| $dA(dC)_{49}$: | ACC CCC CCC CCC CCC CCC CCC CCC CCC CCC CCC CCC CCC CCC CCC CCC CCC CC 3′ | 50.0 | 1.4 | 1.5 | 4957 | 4 |
| $dCdA(dC)_{48}$: | CAC CCC CCC CCC CCC CCC CCC CCC CCC CCC CCC CCC CCC CCC CCC CCC CCC CC 3′ | 51.5 | 0.9 | 0.6 | 5090 | 6 |
| $(dC)_2dA(dC)_{47}$: | CCA CCC CCC CCC CCC CCC CCC CCC CCC CCC CCC CCC CCC CCC CCC CCC CCC CC 3′ | 49.8 | 1.1 | 1.1 | 4076 | 4 |
| $dT(dA)_{49}$: | TAA AAA AAA AAA AAA AAA AAA AAA AAA AAA AAA AAA AAA AAA AAA AAA AAA AA 3′ | 46.6 | 1.2 | 0.7 | 2408 | 4 |
| $dAdT(dA)_{48}$: | ATA AAA AAA AAA AAA AAA AAA AAA AAA AAA AAA AAA AAA AAA AAA AAA AAA AA 3′ | 54.4 | 1.4 | 0.9 | 4760 | 5 |
| $(dA)_2dT(dA)_{47}$: | AAT AAA AAA AAA AAA AAA AAA AAA AAA AAA AAA AAA AAA AAA AAA AAA AAA AA 3′ | 60.7 | 1.6 | 1.2 | 2203 | 4 |
| $dA(dT)_{49}$: | ATT TTT TTT TTT TTT TTT TTT TTT TTT TTT TTT TTT TTT TTT TTT TTT TTT TT 3′ | 55.1 | 1.0 | 1.0 | 2010 | 5 |
| $dTdA(dT)_{48}$: | TAT TTT TTT TTT TTT TTT TTT TTT TTT TTT TTT TTT TTT TTT TTT TTT TTT TT 3′ | 43.8 | 0.9 | 1.4 | 2218 | 4 |
| $(dT)_2dA(dT)_{47}$: | TTA TTT TTT TTT TTT TTT TTT TTT TTT TTT TTT TTT TTT TTT TTT TTT TTT TT 3′ | 42.3 | 1.0 | 1.3 | 1430 | 3 |
| $dG(dA)_{49}$: | GAA AAA AAA AAA AAA AAA AAA AAA AAA AAA AAA AAA AAA AAA AAA AAA AAA AA 3′ | 61.9 | 1.9 | 0.7 | 4036 | 5 |
| $dAdG(dA)_{48}$: | AGA AAA AAA AAA AAA AAA AAA AAA AAA AAA AAA AAA AAA AAA AAA AAA AAA AA 3′ | 63.2 | 1.6 | 0.3 | 4213 | 3 |
| $(dA)_2dG(dA)_{47}$: | AAG AAA AAA AAA AAA AAA AAA AAA AAA AAA AAA AAA AAA AAA AAA AAA AAA AA 3′ | 62.5 | 1.9 | 0.8 | 4461 | 3 |

Table contains sequence (second column) and associated information (remaining columns) of DNA hairpins with different tail sequences when examined with MspA at 180 mV. We additionally show the resulting count-weighted mean of the residual current Gaussian mean, the count-weighted mean of the residual current Gaussian width, the standard error in the mean of the Gaussian mean between a number of experiments, the total number of observed translocations (#transloc), and the number of different experiments (#exp) with each.

Derrington et al. www.pnas.org/cgi/doi/10.1073/pnas.1001831107

**Table S2. Information for hairpin DNA with different duplexes examined with MspA**

| | Hairpin Sequences | | | | | | | |
|---|---|---|---|---|---|---|---|---|
| Duplex | TAIL | #bp | GC% | mean of Gauss mean of $I_{res}$(pA) | mean of Gauss width of $I_{res}$ (pA) | s.e.m. of Gauss means (pA) | # transloc. | # exp |
| 5′ TCT GGC TCT GTT GCT CTC TCG CAA CAG AGC CAG A | $(dA)_{50}$-3′ | 14 | 57 | 70.8 | 8.1 | 4.5 | 2616 | 4 |
| 5′ CCT GGC TCT GTT GCT CTC TCG CAA CAG AGC CAG G | $(dA)_{50}$-3′ | 14 | 64 | 76.5 | 8.4 | 1.2 | 3417 | 4 |
| 5′ ACT GGC TCT GTT GCT CTC TCG CAA CAG AGC CAG T | $(dA)_{50}$-3′ | 14 | 57 | 63.6 | 1.9 | 0.6 | 3967 | 4 |
| 5′ GCC GGC TCT GGT GCT CTC TCG CAC CAG AGC CGG C | $(dA)_{50}$-3′ | 14 | 79 | 67.5 | 0.2 | 0.5 | 1819 | 3 |
| 5′ GCT GTC TGT TGC TCT CTC GCA ACA GAC AGC | $(dA)_{50}$-3′ | 12 | 58 | 66.0 | 1.5 | 2.3 | 3583 | 3 |
| 5′ GCT CTG TTG CTC TCT CGC AAC AGA GC | $(dA)_{50}$-3′ | 10 | 60 | 67.6 | 1.5 | 2.0 | 5305 | 6 |
| 5′ GCT GTT GCT CTC TCG CAA CAG C | $(dA)_{50}$-3′ | 8 | 63 | 68.4 | 1.9 | 1.9 | 4413 | 6 |

Caption same as Table S1 but for varied hairpin duplex sequences using 180 mV. The top three entries (light blue) in the table indicate that the terminal base-pair adjacent to the hairpin-tail affects the residual current. We note that when the 5′ end base of the hairpin is a purine the residual current has a similar value and width. When the 5′ end base is a pyrimidine, the residual current is higher and broader. The length and composition of the hairpin duplex weakly influences the residual current, as indicated by the lower four (orange) entries in the table. The slight increase in residual current when decreasing the length of the hairpin is likely due a reduction in access resistance to MspA's constriction.

**Table S3. Mean and s.d. of the average values of levels from multiple translocation of the 3′-ATGC-5′ DI analyte**

| DNA 3′ ATGC 5′ | | Level Residual Currents (pA) | | | |
|---|---|---|---|---|---|
| Vapp = 180 mV, # exp = 5 | | Level order | | | |
| Associated base | *N* | First | Second | Third | Fourth |
| ATGC | 175 | 65.4 ± 2.1 | 45.7 ± 1.9 | 62.1 ± 2.5 | 47.7 ± 2.6 |
| ATG | 268 | 65.9 ± 2.1 | 45.8 ± 2.3 | 60.9 ± 3.4 | |
| TGC | 76 | 44.7 ± 2.4 | 61.7 ± 2.7 | 48.1 ± 2.7 | |
| AT | 563 | 65.9 ± 3.0 | 47.1 ± 3.0 | | |
| TG | 109 | 44.6 ± 2.1 | 62.4 ± 3.6 | | |
| Vapp = 160 mV, # exp = 3 | | | | | |
| ATGC | 66 | 54.4 ± 1.6 | 36.0 ± 2.0 | 50.2 ± 2.2 | 37.4 ± 1.8 |
| ATG | 65 | 54.1 ± 1.2 | 35.6 ± 2.5 | 49.3 ± 2.9 | |
| TGC | 8 | 31.3 ± 12.9 | 42.1 ± 17.1 | 32.6 ± 13.5 | |
| AT | 189 | 53.7 ± 2.0 | 36.3 ± 2.8 | | |
| TG | 36 | 36.4 ± 3.5 | 51.0 ± 2.8 | | |
| Vapp = 140 mV, # exp = 3 | | | | | |
| ATGC | 44 | 41.3 ± 1.8 | 23.9 ± 1.1 | 37.4 ± 1.7 | 27.4 ± 1.7 |
| ATG | 47 | 41.3 ± 1.3 | 23.5 ± 0.9 | 36.6 ± 2.1 | |
| TGC | 26 | 24.7 ± 3.4 | 37.7 ± 3.7 | 27.5 ± 5.2 | |
| AT | 132 | 40.8 ± 1.9 | 23.9 ± 2.0 | | |
| TG | 30 | 25.9 ± 2.4 | 39.2 ± 3.3 | | |

Events containing four levels were identified to be the complete sequence 3′-ATGC-5′, while current traces with three or two levels were identified to be order-preserved subsets of the 3′-ATGC-5′ sequence. We give also the total number of associated sequence or sequence subset given (N). Results are for applied voltages (Vapp), 180 mV, 160 mV and 140 mV and with the number of experiments (#exp) done for each DNA construct given for each voltage.

**Table S4. Mean and s.d. of the average values of levels from multiple translocation of the 3′-TACG-5′ DI analyte**

| DNA 3′ TACG 5′ | | Level Residual Currents (pA) | | | |
|---|---|---|---|---|---|
| Vapp = 180 mV, # exp = 5 | | Level order | | | |
| Associated base | *N* | First | Second | Third | Fourth |
| TACG | 101 | 43.4 ± 0.7 | 61.4 ± 2.4 | 47.9 ± 1.7 | 59.8 ± 2.6 |
| TAC | 181 | 43.4 ± 1.3 | 62.0 ± 2.3 | 48.3 ± 2.8 | |
| ACG | 20 | 58.0 ± 13.9 | 44.5 ± 10.7 | 56.8 ± 13.7 | |
| TA | 235 | 44.0 ± 2.3 | 60.1 ± 3.5 | | |
| CG | 24 | 61.3 ± 3.1 | 46.8 ± 3.0 | | |
| Vapp = 160 mV, # exp = 3 | | | | | |
| TACG | 61 | 33.3 ± 0.8 | 51.5 ± 1.8 | 38.9 ± 1.4 | 49.3 ± 2.6 |
| TAC | 110 | 33.2 ± 1.7 | 51.7 ± 1.6 | 39.3 ± 2.1 | |
| ACG | 17 | 53.9 ± 2.7 | 38.8 ± 1.6 | 49.8 ± 2.2 | |
| TA | 90 | 33.8 ± 2.9 | 50.0 ± 1.9 | | |
| CG | 19 | 52.5 ± 2.7 | 38.6 ± 3.5 | | |
| Vapp = 140 mV, # exp = 3 | | | | | |
| TACG | 29 | 22.3 ± 7.6 | 38.6 ± 13.2 | 27.6 ± 9.4 | 34.7 ± 12.0 |
| TAC | 54 | 20.5 ± 8.3 | 34.6 ± 14.2 | 25.7 ± 10.5 | |
| ACG | 5 | 21.4 ± 30.1 | 14.6 ± 20.5 | 17.6 ± 24.7 | |
| TA | 30 | 23.2 ± 9.1 | 36.3 ± 13.9 | | |
| CG | 11 | 30.2 ± 20.6 | 20.9 ± 14.3 | | |

Caption as for Table S3.

**Table S5. Mean and s.d. of the average values of levels from multiple translocation of the blind DI sequence, which was determined to be 3′-GTCAC-5′**

| DNA 3′ CACTG 5′ | | Level Residual Currents (pA) | | | | |
|---|---|---|---|---|---|---|
| Vapp = 180 mV, # exp = 3 | | Level order | | | | |
| Associated base | *N* | First | Second | Third | Fourth | Fifth |
| GTCAC | 160 | 61.1 ± 5.1 | 41.7 ± 4.4 | 49.6 ± 4.7 | 62.5 ± 5.6 | 48.8 ± 4.7 |
| GTCA | 140 | 61.4 ± 1.6 | 42.4 ± 3.0 | 49.9 ± 2.6 | 62.0 ± 2.9 | |
| TCAC | 32 | 40.1 ± 10.8 | 47.0 ± 12.6 | 59.2 ± 15.7 | 46.6 ± 12.5 | |
| GCAC | 1227 | 61.4 ± 1.7 | 46.4 ± 1.8 | 62.5 ± 2.1 | 48.6 ± 1.9 | |
| GTAC | 1206 | 61.5 ± 1.6 | 45.9 ± 2.1 | 62.6 ± 2.1 | 49.0 ± 2.1 | |
| Vapp = 160 mV, # exp = 3 | | | | | | |
| GTCAC | 127 | 48.7 ± 4.5 | 31.9 ± 3.5 | 38.2 ± 3.8 | 50.1 ± 4.9 | 38.3 ± 3.9 |
| GTCA | 50 | 48.5 ± 7.0 | 31.8 ± 5.0 | 38.3 ± 5.8 | 49.7 ± 7.5 | |
| TCAC | 15 | 27.2 ± 14.2 | 31.8 ± 16.6 | 41.1 ± 21.3 | 31.6 ± 16.4 | |
| GCAC | 694 | 49.3 ± 1.3 | 35.7 ± 1.7 | 50.6 ± 1.7 | 38.2 ± 1.8 | |
| GTAC | 153 | 49.3 ± 1.2 | 35.2 ± 1.6 | 50.6 ± 1.9 | 38.2 ± 1.8 | |
| Vapp = 140 mV, # exp = 3 | | | | | | |
| GTCAC | 112 | 38.2 ± 0.6 | 23.4 ± 0.8 | 28.9 ± 0.7 | 39.8 ± 1.9 | 29.2 ± 1.5 |
| GTCA | 27 | 36.0 ± 7.6 | 22.7 ± 4.7 | 28.3 ± 5.8 | 37.8 ± 7.9 | |
| TCAC | 30 | 22.1 ± 6.1 | 27.2 ± 7.5 | 37.1 ± 10.2 | 27.5 ± 7.6 | |
| GCAC | 142 | 38.0 ± 3.4 | 26.1 ± 2.5 | 39.6 ± 3.9 | 28.9 ± 2.9 | |
| GTAC | 145 | 37.9 ± 3.4 | 25.7 ± 2.5 | 39.5 ± 3.9 | 28.9 ± 2.9 | |

Caption as for Table S3. The current traces for this sequence had five observed levels; we present results from residual currents containing five or four levels.